Exciting efficient oscillations in nonlinear mechanical systems through Eigenmanifold stabilization

Santina, Cosimo Della; Albu-Schaeffer, Alin

DOI
10.1109/LCSYS.2020.3048228

Publication date
2021

Document Version
Final published version

Published in
IEEE Control Systems Letters

Exciting Efficient Oscillations in Nonlinear Mechanical Systems Through Eigenmanifold Stabilization

Cosimo Della Santina, *Member, IEEE* and Alin Albu-Schaeffer, *Fellow, IEEE*

***Abstract*—Nonlinear modes are a well investigated concept in dynamical systems theory, extending the celebrated modal analysis of linear mechanical systems to nonlinear ones. This letter moves a first step in the direction of combining control theory and nonlinear modal analysis towards the implementation of hyper-efficient oscillatory behaviors in mechanical systems with non-Euclidean metric. Rather than forcing a prescribed evolution, we first investigate the regular behaviors that can be autonomously expressed by the system, and then we design a controller that excites them. A first implementation of this concept is proposed, analyzed, and tested in simulation.**

***Index Terms*—Robotics, stability of nonlinear systems, PID control, flexible structures, control applications.**

I. Introduction

GENERATING stable periodic evolutions in a robotic system is a quite challenging task with practically meaningful applications - as for example pick and place, and locomotion. It is therefore not surprising that it attracted so much attention from both robotics and control theory fields. The challenge has been attacked for weakly underactuated mechanical systems by using virtual holonomic constraints in [1]. The application of this theory to bipedal locomotion is investigated in [2]. Differential Positivity - extending Contraction analysis to periodic orbits [3] - is applied in [4] to study nonlinear oscillations of a pendulum. Immersion and invariance technique is used in [5] to realize a feedback equivalence of the original system with a low dimensional dynamics having a single attractive orbit. Energy shaping of a Mexican hat field is combined with damping injection in [6], for stabilizing a closed orbit identified by the local minima of the function.

Motivated by the same premises, the robotics community has put substantial effort in developing new kinds of robotic systems which are more suited for presenting oscillatory behaviors. This is typically done by shaping the potential field acting on the mechanical system - e.g., though the introduction of carefully designed elastic elements, leading to the so-called articulated soft robots [7]. Auxiliary springs are optimally tuned to reduce the control effort required for tracking specific trajectories in [8]–[10]. Several mechanisms to realize complex and possibly adjustable stiffness characteristics have been also proposed [11], [12].

Having designed these new robots for efficiency, naturally leads to rethinking control goals. Within this context, implementing stable periodic motions is not enough anymore. We want instead to achieve simultaneously stability end efficiency. Numerical [13] and analytical [14] optimization have been used to implement efficient oscillations in low dimensional robots. In [15] authors propose a controller which matches the spring loaded inverted pendulum to the hybrid zero-dynamics of an asymmetric segmented leg. Adaptive oscillators are also used in this context [16]. Moving to more general systems, [17] proposes to use model based decoupling of the joints dynamics. In [18] virtual holonomic constraints are combined with energy regulation, with the aim of reducing the extent of direct dynamic cancellation operated by the controller. Still, a substantial component of dynamics cancellation is envisaged by all these strategies, which results only in a partial exploitation of the intrinsic dynamics of the robot.

The aim of this letter is to move a step towards reaching a complete exploitation of robot's dynamics, possibly at the cost of reducing the generality of motions that can be realized by the closed loop. We propose to do that by exploiting modal analysis to characterize nonlinear counterparts of the linear eigenspaces, called Eigenmanifolds. Stabilizing these submanifolds of the configuration space by means of feedback control can be seen as a simple and robust way of exciting hyper-efficient nonlinear oscillations in robotic systems. We combine this control action with energy regulation to increase or decrease the amplitude of the oscillations. Fig. 1 presents a sketch of this idea. No model compensation is involved in this technique, which therefore converges to zero control action at steady state. We refer to this behavior as hyper–efficient.

Manuscript received September 4, 2020; revised November 26, 2020; accepted December 14, 2020. Date of publication December 30, 2020; date of current version March 8, 2021. This work was supported by the European Union ERC Project under Grant 835284 (M-Runners). Recommended by Senior Editor F. Dabbene. *(Corresponding author: Cosimo Della Santina.)*

Cosimo Della Santina is with the Institute of Robotics and Mechatronics, German Aerospace Center (DLR), 82234 Oberpfaffenhofen, Germany, also with the Informatics and Mathematics Department, Technical University of Munich, 80333 Garching bei München, Germany, and also with Cognitive Robotics Department, TU Delft, 2628 CD Delft, The Netherlands (e-mail: cosimo.dellasantina@dlr.de).

Alin Albu-Schaeffer is with the Institute of Robotics and Mechatronics, German Aerospace Center (DLR), 82234 Oberpfaffenhofen, Germany, and also with the Informatics and Mathematics Department, Technical University of Munich, 80333 Garching bei München, Germany (e-mail: alin.albu-schaeffer@dlr.de).

Digital Object Identifier 10.1109/LCSYS.2020.3048228

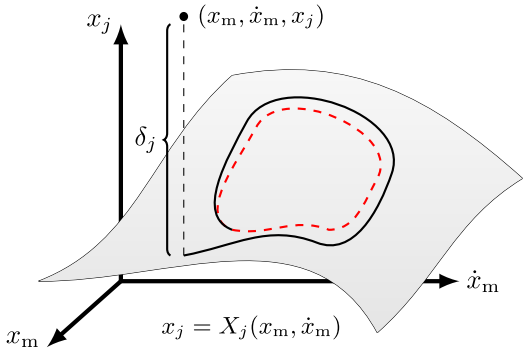

Fig. 1. We propose to generate efficient cyclic motions in nonlinear mechanical systems by stabilizing the nonlinear counterpart of the linear Eigenspace, called Eigenmanifold. These surfaces are built as a collection of all the regular oscillatory behaviors that the system can present in open loop, organized per energy levels. A section of the Eigenmanifold with main quantities highlighted is shown in the picture.

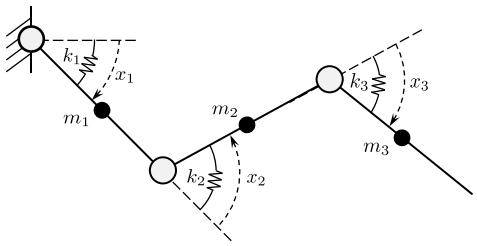

Fig. 2. A picture of the RRR robot with parallel elasticity considered in this letter. The masses are positioned in the center of each link, and the link inertia is neglected. Torques (not shown in picture) can be independently applied at each joint.

Due to space limitations, the goal of this letter is to present this idea in its most basic form, so to focus on its core principles rather than on (possibly important) technicalities, which will be tackled in future work. To this end, we also simplify the problem by considering conservative and fully actuated systems. Moreover we focus on the derivation of local (in the sense of small distances from the manifold) results, rather than global. We believe that none of these hypotheses is essential, and we are confident that will be successful in relaxing them in future work.

II. Nonlinear Modes of a Multi-Body System

Linear modal analysis is a priceless tool in the letter of linear mechanical systems, allowing to describe regular oscillations in apparently complex and large scale interconnections of masses and springs. Over the past century, several generalizations of normal modes to the nonlinear case have been proposed. We refer to [19] for a survey on the topic. However, the large part of these works dealt with interconnections of masses through nonlinear springs, neglecting any configuration-dependent inertia term. This is clearly not suited for the robotic case. In recent work [20], we proposed an extension of this theory to the general smooth conservative case. We showed there that a rich structure of regular evolutions persist, even when we leave the Euclidean world.

A. Dynamical Model

Consider the coordinate expression of the dynamics of a nonlinear mechanical system

$$M(x)\ddot{x} + C(x,\dot{x})\dot{x} + \frac{\partial V(x)}{\partial x} = \tau, \tag{1}$$

where $x \in \mathbb{R}^n$ are the joint coordinates of the robot, $\dot{x}, \ddot{x}$ their time derivatives, $M(x) \in \mathbb{R}^{n\times n}$ is the inertia matrix, $C(x,\dot{x}) \in \mathbb{R}^{n\times n}$ collects Coriolis and centrifugal terms, $V(x) \in \mathbb{R}$ is the potential (for example including gravity and elastic contributions). For the sake of space, we also use the notation $f(x,\dot{x}) = -M^{-1}(x)(C(x,\dot{x})\dot{x} + \frac{\partial V(x)}{\partial x})$ and $g(x) = M^{-1}(x)$. The state of (1) is $(x,\dot{x}) \in \mathbb{R}^{2n}$, and its total energy is

$$E(x,\dot{x}) = \frac{1}{2}\dot{x}^\mathrm{T} M(x)\dot{x} + V(x). \tag{2}$$

B. Definition

We provide here a simplified coordinate dependent definition of the Eigenmanifold. We point to [20, Sec. 7] for the formal coordinate-free definition. We start by assuming that $x_\mathrm{eq} \in \mathbb{R}^n$ exists such that $V(x_\mathrm{eq})$ is a minimum - i.e., we assume the existence of a stable equilibrium configuration for (1) with $\tau = 0$. We select one eigenspace of dimension two ES of the linearized system at x_eq. Since (1) is conservative, we can express the eigenspace as follows [20, Sec. 2]

$$ES = \mathrm{Span}\{(c,\ 0),\ (0,\ c)\}, \tag{3}$$

where $c \in \mathbb{R}^n$ is an unit vector pointing the direction of oscillations. To simplify the notation, we introduce the modal coordinates $x_\mathrm{m} = c^\mathrm{T}x$ and $\dot{x}_\mathrm{m} = c^\mathrm{T}\dot{x}$. Any point in ES can therefore be unequivocally expressed as a linear combination of these two variables. We can therefore more concisely say that $(x_\mathrm{m}, \dot{x}_\mathrm{m}) \in ES \simeq \mathbb{R}^2$. When the linear system is initialized in ES, it evolves without ever exiting the eigenspace, following the sinusoidal oscillatory pattern $x_\mathrm{m}(t) = A\sin(\lambda^2 t + \phi)$, where λ is the eigenvalue associated to ES, and $A, \phi \in \mathbb{R}$ are two constants with value defined by the initial conditions. The trajectories $(x_\mathrm{m}, \dot{x}_\mathrm{m})$ span all ES when varying A from 0 to ∞. Eigenspaces can therefore be seen as a collection of all the regular trajectories that the system can perform. Increasing values of A are unequivocally associated to increasing values of energy.

Moving from the linear to the nonlinear case, the plane ES bends into a surface with the same dimension, that we call Eigenmanifold. More specifically we say that a 2-dimensional submanifold $\mathfrak{M}$ of the configuration space $\mathbb{R}^{2n}$ is an Eigenmanifold, if it is a collection of periodic orbits with increasing energy levels, i.e., each $x(t)$ such that $\dot{x}(0) = 0$ and $(x(0), 0) \in \mathfrak{M}$ is periodic and it is fully contained in $\mathfrak{M}$. Also we require that $(x_\mathrm{eq}, 0) \in \mathfrak{M}$. Finally, we want the trajectories to be homeomorphic to a segment when projected in configuration space. We refer to [20] for a discussion about why these conditions directly extend the linear case. Therefore, as for the linear Eigenspaces, the Eigenmanifolds characterize all the regular oscillatory behaviors - continuously growing from an equilibrium - that the nonlinear mechanical system can perform without any (long term) control intervention.

In [20, Sec. 9.4], we show that two functions $X : ES \to \mathbb{R}^n$ and $\dot{X} : ES \to \mathbb{R}^n$ can always be found - at least locally - such that the Eigenmanifold is directly and equivalently defined in coordinates as

$$\mathfrak{M} = \left\{(x,\dot{x}) \in \mathbb{R}^{2n},\ \text{s.t.}\, X(x_\mathrm{m}, \dot{x}_\mathrm{m}) = x, \dot{X}(x_\mathrm{m}, \dot{x}_\mathrm{m}) = \dot{x}\right\},$$

where $(x_\mathrm{m}, \dot{x}_\mathrm{m})$ are the coordinates of ES defined above. Note that to be coherent with this definition the embeddings should be such that $(c^\mathrm{T}X, c^\mathrm{T}\dot{X})$ is the identity function. Also, we assume the Jacobian of $(X,\dot{X}) - (x,\dot{x})$ to have everywhere the maximum rank possible. Therefore $(X,\dot{X}) = (x,\dot{x})$ effectively constraints $2n-2$ degrees of freedom out of $\mathbb{R}^{2n}$. Thus,

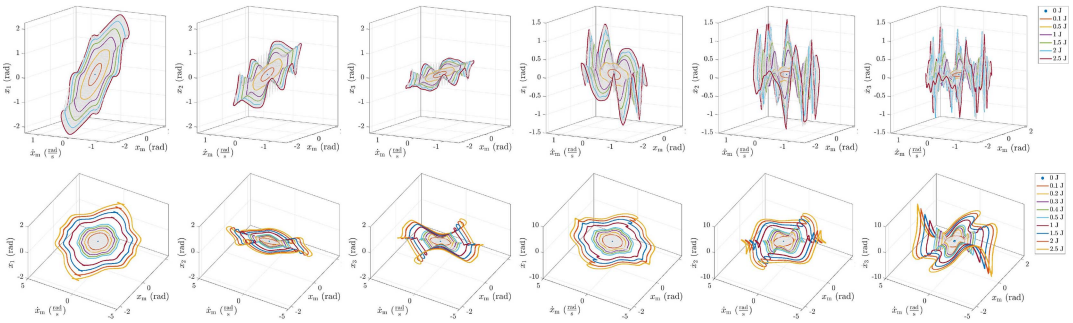

Fig. 3. Two Eigenmanifolds of the considered RRR robot with parallel elasticity, represented as level curves of $(X, \dot{X}) = (x, \dot{x})$. The two rows correspond to 1st and 2nd modes respectively. Each column shows the appropriate level set of a different element of $(X, \dot{X})$. We also show examples of modal evolutions depicted by solid lines, with color coded energy level.

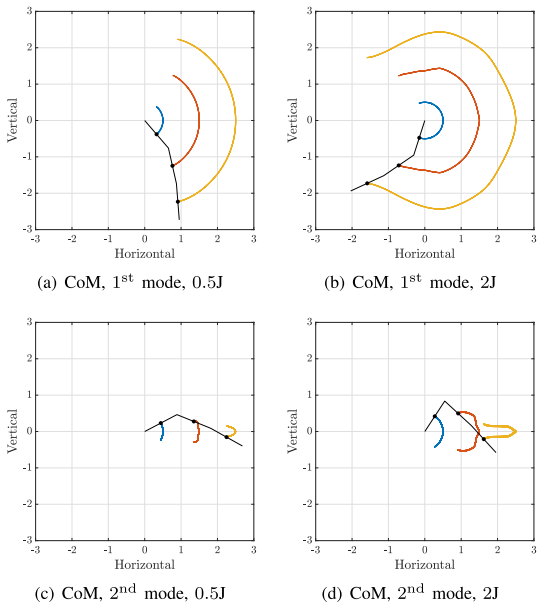

(a) CoM, 1st mode, 0.5J (b) CoM, 1st mode, 2J

(c) CoM, 2nd mode, 0.5J (d) CoM, 2nd mode, 2J

Fig. 4. Examples of nonlinear modes extending the first two linear modes, for a 3-link serial robot. Evolutions of the centers of mass are shown. A schematic representation of the robot in one of the two zero velocity configurations is also superimposed - with the black dots indicating the centers of mass.

this definition of $\mathfrak{M}$ is coherent with the intrinsic one given before since the equality constraints define a two dimensional sub-manifold according to the implicit function theorem. The function $(X, \dot{X}) : ES \to \mathbb{R}^{2n}$ is called coordinate expression of the embedding of $\mathfrak{M}$ in the state space. Given ES we can always find an approximation of the functions $(X, \dot{X})$ identifying its nonlinear extension $\mathfrak{M}$, as discussed in [20, Sec. 9.1]. This result can be achieved with any level of precision. Thus, for the sake of conciseness, we will consider the embedding to be exactly known in the rest of theoretical derivation. This hypothesis will be removed in the simulations.

C. Example: RRR Robot With Parallel Elasticity

Consider the planar robot in Fig. 2. Its dynamics can be described as in Section II-A, where $x = (x_1, x_2, x_3)$ are the joint coordinates. The energy (2) is specified by $V(x) = x^{\mathrm{T}}x/2$ and the inertia matrix $M(x)$ is the usual one for RRR robots with mass concentrated in the middle of the link. Stiffnesses, masses, and lengths are chosen unitary. The unique equilibrium (global minimum of V) is in $(0, 0, 0)$, i.e., when the robot is in a straight configuration.

The three eigenspaces of the linearized system in this equilibrium are identified by c equal to (i) $(0.8781, 0.4604, 0.1306)$, (ii) $(0.4570, -0.7258, -0.5141)$, (iii) $(0.1419, -0.5111, 0.8477)$, organized by increasing values of oscillation frequency. We use the algorithm in [20] to evaluate the manifold $\mathfrak{M}$ extending the linear modes. The third mode extends into an highly numerically unstable oscillation, which gets not identifiable with our current algorithms already at low energies. Therefore, we do not discuss this Eigenmanifold further in this letter.

The Eigenmanifolds extending modes (i) and (ii) are shown in Fig. 3. Note that the modal variables x_{m} and $\dot{x}_{\mathrm{m}}$ are chosen here as the directions pointed by the linear modes of which the eigenmanifold is an extension. The gray surface shows the eigenmanifold, as resulting from the parametrization $(X, \dot{X})$. The first mode extends up to high energies, and the parametrization can successfully cover all the investigated area. Also the second mode extends up to high energies. Yet, the parametrization can reach only up to 0.5J, due to the self folding of the trajectories when observed through X and $\dot{X}$. The evolutions of the robot's centers of mass are shown in Fig. 4. Although corresponding coordinate evolutions in time cannot be shown here for the sake of space, examples will be provided in Section III-E.

III. Control Strategy

Suppose to have identified all the Eigenmanifolds of a mechanical system, and selected among them the one that implements a desired behavior. Our goal is now to develop controllers that can excite the nonlinear normal modes contained in this manifold. If we succeed in this task, the result is the execution of hyper-efficient nonlinear oscillations. We propose here two feedback loops, one making the selected Eigenmanifold a local attractor (Sections III-A–III-C), and the other selecting a single mode within the family of available ones by means of energy regulation (Section III-D). Once both the Eigenmanifold and the desired energy level are reached, we can leave the system free to evolve according to its own dynamics. Fig. 1 summarizes these ideas.

A. Manifold Stabilization: Goals

Consider an algebraic feedback, function of the state $(x, \dot{x})$. Its goal is to make the system evolutions $x(t)$ converge to the manifold $\mathfrak{M}$. This request can be formalized by asking that (see coordinate-dependent definition, Section II-B)

$$\lim_{t\to\infty} (X(x_{\mathrm{m}}, \dot{x}_{\mathrm{m}}) - x) = 0, \quad \lim_{t\to\infty} \left(\dot{X}(x_{\mathrm{m}}, \dot{x}_{\mathrm{m}}) - \dot{x}\right) = 0. \quad (4)$$

We define the distances from the manifold in position $\delta \in \mathbb{R}^{n-1}$ and in velocity $\xi \in \mathbb{R}^{n-1}$ as part of the following change of coordinates

$$\begin{aligned}(x_\mathrm{m}, \delta) &= \big(c^\mathrm{T}x,\ c_\perp^\mathrm{T}\big(x - X(c^\mathrm{T}x, c^\mathrm{T}\dot{x})\big)\big),\\ (\dot{x}_\mathrm{m}, \xi) &= \big(c^\mathrm{T}\dot{x},\ c_\perp^\mathrm{T}\big(\dot{x} - \dot{X}(c^\mathrm{T}x, c^\mathrm{T}\dot{x})\big)\big),\end{aligned} \tag{5}$$

where $c_\perp \in \mathbb{R}^{n\times n-1}$ is such that $c_\perp^\mathrm{T}c = 0$ and $c_\perp^\mathrm{T}c_\perp = I$. Note that ξ is not the time derivative of δ. We will further discuss this point later in this section.

Considering that, as discussed in Section II-B, $c^\mathrm{T}X(x_\mathrm{m}, \dot{x}_\mathrm{m}) = c^\mathrm{T}x$ and $c^\mathrm{T}\dot{X}(x_\mathrm{m}, \dot{x}_\mathrm{m}) = c^\mathrm{T}\dot{x}$ for all $(x, \dot{x}) \in \mathbb{R}^{2n}$, and that $[c_\perp\ c]$ is an orthogonal matrix, yields

$$X(x_\mathrm{m}, \dot{x}_\mathrm{m}) - x = c_\perp\delta, \quad \dot{X}(x_\mathrm{m}, \dot{x}_\mathrm{m}) - \dot{x} = c_\perp\xi. \tag{6}$$

As a consequence we can recast (4) as

$$\lim_{t\to\infty}(\delta, \xi) = (0, 0). \tag{7}$$

Finally, the feedback must also be manifold preserving, i.e., $\mathfrak{M}$ is also an Eigenmanifold of the closed loop. This can be achieved through a feedback that vanishes on the manifold

$$\tau(x, \dot{x})|_{(x,\dot{x})\in\mathfrak{M}} = 0. \tag{8}$$

B. Manifold Stabilization: Tangency Constraints

Whenever possible, we will leverage on the intrinsic properties of the Eigenmanifold to solve the control problem. A major characteristics of $\mathfrak{M}$ is to be invariant, meaning that if $(x(0), \dot{x}(0)) \in \mathfrak{M}$, then $(x(t), \dot{x}(t)) \in \mathfrak{M}$ for all t. This property can be alternatively formulated in terms of variations of distances from the manifold

$$\left(\frac{\mathrm{d}}{\mathrm{d}t}\big((x, \dot{x}) - \big(X, \dot{X}\big)\big)\right)\Bigg|_{(x,\dot{x})\in\mathfrak{M}} = 0, \tag{9}$$

which says that while evolving on the manifold, the distance from $\mathfrak{M}$ does not increase in time. We expand separately the position and velocity parts of (9) by using the chain rule, obtaining the following equations

$$\dot{X} - \frac{\partial X}{\partial x_\mathrm{m}}\dot{x}_\mathrm{m} - \frac{\partial X}{\partial \dot{x}_\mathrm{m}}c^\mathrm{T}f(X, \dot{X}) = 0, \tag{10}$$

$$f(X, \dot{X}) - \frac{\partial \dot{X}}{\partial x_\mathrm{m}}\dot{x}_\mathrm{m} - \frac{\partial \dot{X}}{\partial \dot{x}_\mathrm{m}}c^\mathrm{T}f(X, \dot{X}) = 0. \tag{11}$$

C. Manifold Stabilization: Control Derivation

Output regulation techniques, such as multivariate [21] or trasverse [22] feedback linearization, could be seen as stabilizing the manifold identified by the level sets of the output - which in this case would be the zero level set of $(X, \dot{X}) - (x, \dot{x})$. The opportunity of using these techniques will be investigated in future work. Here, we aim at achieving the control goal by relying very sparsely on model cancellation. More specifically, we wish to see if a simple PD-like action can make the Eigenmanifold an attractor of the closed loop system. Therefore, we propose the control candidate

$$\begin{aligned}\tau(x, \dot{x}) &= +M(x)\big(\alpha_\mathrm{P}(x - X(x_\mathrm{m}, \dot{x}_\mathrm{m})) + \alpha_\mathrm{D}\big(\dot{x} - \dot{X}(x_\mathrm{m}, \dot{x}_\mathrm{m})\big)\big)\\ &= -M(x)c_\perp(\alpha_\mathrm{P}\delta + \alpha_\mathrm{D}\xi),\end{aligned} \tag{12}$$

where α_P and α_P are two scalar gains. The second step is yielded by (6).

With the aim of connecting the velocity part of the distance from the manifold ξ to the derivative of the position part, we start by evaluating the latter from (5), obtaining $\dot{\delta} = c_\perp^\mathrm{T}\dot{x} - c_\perp^\mathrm{T}(\frac{\partial X}{\partial x_\mathrm{m}}\dot{x}_\mathrm{m} + \frac{\partial X}{\partial \dot{x}_\mathrm{m}}c^\mathrm{T}(f(x, \dot{x}) + M^{-1}(x)\tau))$, where we used the chain rule to express the time derivative of X. Consider now that

$$c^\mathrm{T}M^{-1}(x)\tau = c^\mathrm{T}c_\perp(\alpha_\mathrm{P}\delta + \alpha_\mathrm{D}\xi) = 0. \tag{13}$$

Combining (5), (6), (10), and (13) we obtain

$$\dot{\delta} = \xi - c_\perp^\mathrm{T}\frac{\partial X}{\partial \dot{x}_\mathrm{m}}c^\mathrm{T}\big(f(X + c_\perp\delta, \dot{X} + c_\perp\xi) - f(X, \dot{X})\big), \tag{14}$$

which for small displacements from the manifold, we can approximate by means of standard multivariate Taylor first order expansion

$$\dot{\delta} \simeq \xi - c_\perp^\mathrm{T}\frac{\partial X}{\partial \dot{x}_\mathrm{m}}c^\mathrm{T}\left(\left(\frac{\partial f}{\partial x}\right)_\mathfrak{M}c_\perp\delta + \left(\frac{\partial f}{\partial \dot{x}}\right)_\mathfrak{M}c_\perp\xi\right). \tag{15}$$

where we use the suffix $\mathfrak{M}$ to say that $(x, \dot{x}) \in \mathfrak{M}$, i.e., that $(x, \dot{x}) = (X, \dot{X})$. We can now invert the relationship

$$\xi \simeq \left(I - c_\perp^\mathrm{T}\frac{\partial X}{\partial \dot{x}_\mathrm{m}}c^\mathrm{T}\left(\frac{\partial f}{\partial \dot{x}}\right)_\mathfrak{M}c_\perp\right)^{-1}\left(\dot{\delta} + c_\perp^\mathrm{T}\frac{\partial X}{\partial \dot{x}_\mathrm{m}}c^\mathrm{T}\left(\frac{\partial f}{\partial x}\right)_\mathfrak{M}c_\perp\delta\right). \tag{16}$$

This assures that if $(\delta, \dot{\delta}) \to (0, 0)$ then our control goal (7) is fulfilled. We then aim at proving the first part of the logical implication by extracting the second derivative of the displacement from (14)

$$\begin{aligned}\ddot{\delta} = {}& c_\perp^\mathrm{T}f(x, \dot{x}) + c_\perp^\mathrm{T}M^{-1}(x)\tau(x, \dot{x}) - c_\perp^\mathrm{T}\frac{\mathrm{d}\dot{X}}{\mathrm{d}t}\\ &- c_\perp^\mathrm{T}\frac{\mathrm{d}}{\mathrm{d}t}\left(\frac{\partial X}{\partial \dot{x}_\mathrm{m}}c^\mathrm{T}\big(f(x, \dot{x}) - f(X, \dot{X})\big)\right).\end{aligned} \tag{17}$$

We need now to rewrite everything as function of the new coordinates (5), i.e., removing any explicit dependency on $x, \dot{x}$. To this end, we start with extracting the time derivative of the velocity part of the manifold parametrization

$$\begin{aligned}\frac{\mathrm{d}\dot{X}}{\mathrm{d}t} &= \frac{\partial \dot{X}}{\partial x_\mathrm{m}}\dot{x}_\mathrm{m} + \frac{\partial \dot{X}}{\partial \dot{x}_\mathrm{m}}c^\mathrm{T}\big(f(x, \dot{x}) - M^{-1}(x)\tau(x, \dot{x})\big)\\ &= f(X, \dot{X}) + \frac{\partial \dot{X}}{\partial \dot{x}_\mathrm{m}}c^\mathrm{T}\big(f(x, \dot{x}) - f(X, \dot{X})\big),\end{aligned} \tag{18}$$

where in the second step we used (11) and (13). For the sake of space, we consider here a slowly varying mismatch between $\dot{\delta}$ and ξ, at least in the directions orthogonal to the eigenspace - i.e., we neglect the latter term in (17). Note that this hypothesis is imposed for the sake of space, and similar results could be obtained without imposing it by following the same steps. Therefore, combining (17) and (18) yields (remember that $c_\perp^\mathrm{T}c_\perp = I$) $\ddot{\delta} \simeq c_\perp^\mathrm{T}(I - \frac{\partial \dot{X}}{\partial \dot{x}_\mathrm{m}}c^\mathrm{T})(f(x, \dot{x}) - f(X, \dot{X})) - \alpha_\mathrm{P}\delta - \alpha_\mathrm{D}\xi$. Applying again the hypothesis of small displacements from the manifold, the acceleration can be approximated as

$$\begin{aligned}\ddot{\delta} \simeq {}& \left(c_\perp^\mathrm{T}\left(I - \frac{\partial \dot{X}}{\partial \dot{x}_\mathrm{m}}c^\mathrm{T}\right)\left(\frac{\partial f}{\partial x}\right)_\mathfrak{M}c_\perp - \alpha_\mathrm{P}I\right)\delta\\ &+ \left(c_\perp^\mathrm{T}\left(I - \frac{\partial \dot{X}}{\partial \dot{x}_\mathrm{m}}c^\mathrm{T}\right)\left(\frac{\partial f}{\partial \dot{x}}\right)_\mathfrak{M}c_\perp - \alpha_\mathrm{D}I\right)\xi.\end{aligned} \tag{19}$$

Note that the matrices multiplying δ and ξ are functions of $(x_\mathrm{m}, \dot{x}_\mathrm{m})$ only. We can now use (16) to get the following second order dynamics in $\delta, \dot{\delta}, x_\mathrm{m}, \dot{x}_\mathrm{m}$

$$\ddot{\delta} \simeq \kappa(x_\mathrm{m}, \dot{x}_\mathrm{m})\delta + \beta(x_\mathrm{m}, \dot{x}_\mathrm{m})\dot{\delta}, \tag{21}$$

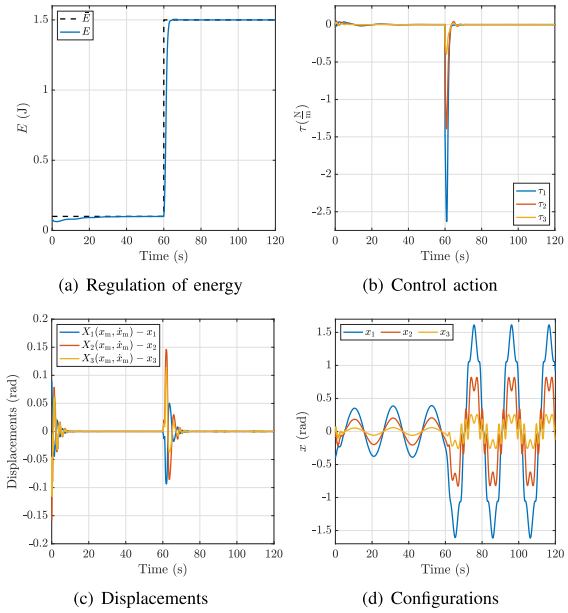

(a) Regulation of energy (b) Control action

(c) Displacements (d) Configurations

Fig. 5. Sequential excitation of two modes contained in the Eigenmanifold extending the first (slowest) Eigenspace. The first oscillation is smaller amplitude and it takes place up to 60s, when higher one starts.

where κ and β are the matrices in (20) shown at the bottom of the page. Proving the stability of (21) requires small gain theorem arguments, which it is beyond the scope of this letter to discuss. Indeed, the evolution $(x_m, \dot{x}_m)$ is in turn function of δ.

Yet, interesting insights can already be taken considering $(\partial(c^T f)/\partial x)_{\mathfrak{M}} \simeq 0$ and $(\partial(c^T f)/\partial \dot{x})_{\mathfrak{M}} \simeq 0$, i.e., $\ddot{x}_m \simeq c^T f(X, \dot{X})$. This condition is always exactly fulfilled in the linear case. Note that the same hypotheses also sensitively simplify (20), nullifying the right hand side of both matrices. In this case x_m can be seen as a time variance, and (21) can be analyzed using standard methods in time varying systems [23]. For example, we can take α_D big enough such that the convergence time of δ is small if compared with the period T of x_m. In this case we can apply averaging technique [24, Sec. 10], resulting in the following sufficient conditions for the asymptotic stability of the origin of (21)

$$\alpha_P > \max_{x_m, \dot{x}_m} \rho\left(\left(I - \frac{\partial \dot{X}}{\partial \dot{x}_m} c^T\right)\left(\frac{\partial f}{\partial \dot{x}}\right)_{\mathfrak{M}}\right),$$
$$\alpha_D > \max_{x_m, \dot{x}_m} \rho\left(\left(I - \frac{\partial \dot{X}}{\partial \dot{x}_m} c^T\right)\left(\frac{\partial f}{\partial \dot{x}}\right)_{\mathfrak{M}}\right), \tag{22}$$

where ρ extracts the maximum eigenvalue of the symmetric part of the argument.

D. Energy Regulation

We design a feedback loop such that the energy $E(x, \dot{x})$ converges to a desired level $\bar{E}$. In this way we can select a single modal oscillation - i.e., the intersection between the constant energy manifold and the Eigenmanifold - and we can increase or decrease the amplitude of the oscillation at will. We start by evaluating the time derivative of (2), which through standard manipulations leads to $\dot{E} = \dot{x}^T M^{-1}(x)\tau(x, \dot{x})$. We can now close the loop so to obtain the desired asymptotic behavior

$$\tau(x, \dot{x}) = \gamma M(x)\big(\bar{E} - E(x, \dot{x})\big)\dot{x}, \tag{23}$$

where $\gamma > 0$ is a gain. This yields the scalar dynamics $\dot{E} = \gamma ||\dot{x}||^2(\bar{E} - E)$. To investigate its steady state behavior we consider the Lyapunov candidate $(\bar{E} - E)^2/2$, with time derivative $-\gamma \|\dot{x}\|^2(\bar{E} - E)^2 \leq 0$. This assures that $\bar{E} - E$ is not increasing, which in turn assures that the state is bounded. Differentiating a second time and applying the Barbalat's lemma [24, Sec. 8.3], we discover that (23) converges to either x_{eq} or to the level set $E(x, \dot{x}) = \bar{E}$. Local stability analysis proves x_{eq} that it is made repulsive by (23). Thus, the manifold $E(x, \dot{x}) = \bar{E}$ is attractive.

E. Example: RRR Robot With Parallel Elasticity (Cont'd)

Consider the system discussed in Section II-C. We use here (12) and (23) to excite the modal oscillations discussed above. We set the control gains to $\alpha_P = 0$, $\alpha_D = 1\frac{1}{s}$, and $\gamma = 1$. The system is always initialized in $x(0) = (-\pi/16, 0, 0)$, and $\dot{x}(0) = 0$. First, we test the strategy under nominal conditions, when trying to regulate modes taken from the first Eigenmanifold. Results are shown in Fig. 5. Two modes are sequentially regulated, the first with $\bar{E} = 0.2$J and the second with $\bar{E} = 1.5$. In both cases, the steady state is reached in few seconds, and with zero final error. Most importantly, the control action drops to zero as soon as the desired mode is reached. The oscillation sustains itself, without any need of injecting extra energy to maintaining it. Note, however, that this is possible only thanks to the non dissipative nature of the mechanical systems under consideration.

Next we test the robustness of the control strategy against model uncertainties. Since we want to put the algorithm under stress, we perturb the only part of (1) appearing explicitly into (12) and (23), i.e., the inertia matrix. Therefore, we simulated the system using a perturbed inertia $\tilde{M}$ which is equal to $0.8M$, where M is the inertia matrix that we used for computations. Coriolis forces are influenced accordingly. Note that $(X, \dot{X})$ is still evaluated with the nominal system. Therefore, this simulation serves also to further test the robustness of the proposed method to uncertain embeddings. We perform two excitations tasks. In the first we excite the mode with $\bar{E} = 1$J, part of the first Eigenmanifold. In the second we excite the one with $\bar{E} = 0.2$J, and being part of the second Eigenmanifold. Results of energy regulations are shown in Figs. 6 (a,b). In both cases the energy converges to a small neighborhood of the desired behavior. Nominal evolutions of the energy are shown for comparison. Finally, the remainder of Fig. 6 shows the joint space evolutions together with the control action. The steady state behavior is still periodic and very similar to the ideal one. Also, the control action drops to very small values after few seconds. The error is not null this time due to the

$$\kappa(x_m, \dot{x}_m) = \left(c_\perp^T\left(I - \frac{\partial \dot{X}}{\partial \dot{x}_m} c^T\right)\left(\frac{\partial f}{\partial x}\right)_{\mathfrak{M}} c_\perp - \alpha_P I\right)\left(I + \left(I - c_\perp^T \frac{\partial X}{\partial \dot{x}_m} c^T\left(\frac{\partial f}{\partial \dot{x}}\right)_{\mathfrak{M}} c_\perp\right)^{-1} c_\perp^T \frac{\partial X}{\partial \dot{x}_m} c^T\left(\frac{\partial f}{\partial x}\right)_{\mathfrak{M}} c_\perp\right)$$
$$\beta(x_m, \dot{x}_m) = \left(c_\perp^T\left(I - \frac{\partial \dot{X}}{\partial \dot{x}_m} c^T\right)\left(\frac{\partial f}{\partial \dot{x}}\right)_{\mathfrak{M}} c_\perp - \alpha_D I\right)\left(I - c_\perp^T \frac{\partial X}{\partial \dot{x}_m} c^T\left(\frac{\partial f}{\partial \dot{x}}\right)_{\mathfrak{M}} c_\perp\right)^{-1} \tag{20}$$

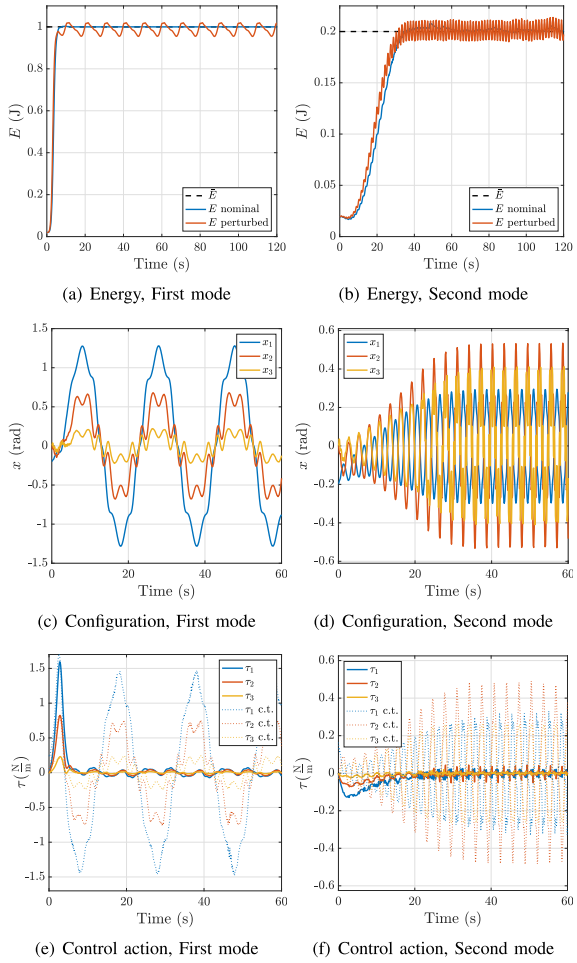

(a) Energy, First mode (b) Energy, Second mode

(c) Configuration, First mode (d) Configuration, Second mode

(e) Control action, First mode (f) Control action, Second mode

Fig. 6. Control performance in presence of uncertainties. The system mass is 80% smaller in simulation than in the model used for control design. Panels (a,b) show the evolution of the energy in nominal and perturbed condition, when regulating the first and the second mode respectively. The reference is shown as a black dashed line. Panels (c,d) report evolution of joint coordinates. Panels (e,f) reports the control action. In the latter plots, also the output of a computed torque controller regulating the same mode when $V = 0$ (i.e., standard approach) is shown as a comparison. This is a pure rigid body motion, since no energy can be stored in the springs.

model mismatching. This analysis - even if preliminary - confirms the effectiveness of the proposed method under uncertain conditions.

IV. Conclusion and Future Work

This letter proposed a method for exciting hyper-efficient oscillations in multi body mechanical systems, by simultaneously regulating Eigenmanifolds and energy levels. Future work will be devoted to developing a global proof of the closed loop stability, assessing theoretically the robustness of the method to non exact embeddings, and dealing with dissipative actions. We believe that differential positivity [3] can be a viable solution for the first two challenges, possibly together with the introduction of a covariant set of coordinates. For what concerns the latter, our preliminary experimental investigations show that dissipation simplifies the excitation of regular oscillation by acting as a stabilizing effect. On a theoretical level dealing with non conservative forces entails two challenges: generalizing the Eigenmanifold concept itself [20, Sec. 10], and devising controller that can generalize (23) so to re-inject the energy lost.

References

[1] M. Maggiore and L. Consolini, "Virtual holonomic constraints for Euler–Lagrange systems," *IEEE Trans. Autom. Control*, vol. 58, no. 4, pp. 1001–1008, Apr. 2013.

[2] B. G. Buss, K. A. Hamed, B. A. Griffin, and J. W. Grizzle, "Experimental results for 3D bipedal robot walking based on systematic optimization of virtual constraints," in *Proc. Amer. Control Conf. (ACC)*, 2016, pp. 4785–4792.

[3] F. Forni and R. Sepulchre, "Differential dissipativity theory for dominance analysis," *IEEE Trans. Autom. Control*, vol. 64, no. 6, pp. 2340–2351, Jun. 2019.

[4] F. Forni and R. Sepulchre, "Differential analysis of nonlinear systems: Revisiting the pendulum example," in *Proc. 53rd IEEE Conf. Decis. Control*, 2014, pp. 3848–3859.

[5] R. Ortega, B. Yi, J. G. Romero, and A. Astolfi, "Orbital stabilization of nonlinear systems via the immersion and invariance technique," *Int. J. Robust Nonlinear Control*, vol. 30, no. 5, pp. 1850–1871, 2020.

[6] B. Yi, R. Ortega, D. Wu, and W. Zhang, "Orbital stabilization of nonlinear systems via mexican sombrero energy shaping and pumping-and-damping injection," *Automatica*, vol. 112, Feb. 2020, Art. no. 108661.

[7] C. D. Santina, M. G. Catalano, and A. Bicchi, *Soft Robots*. Berlin, Germany: Springer, 2020.

[8] U. Mettin, P. X. M. La Hera, L. B. Freidovich, and A. S. Shiriaev, "Parallel elastic actuators as a control tool for preplanned trajectories of underactuated mechanical systems," *Int. J. Robot. Res.*, vol. 29, no. 9, pp. 1186–1198, 2010.

[9] J. Pen, W. Caarls, M. Wisse, and R. Babuska, "Evolutionary co-optimization of control and system parameters for a resonating robot arm," in *Proc. IEEE Int. Conf. Robot. Autom.*, 2013, pp. 4195–4202.

[10] L. F. van der Spaa, W. J. Wolfslag, and M. Wisse, "Unparameterized optimization of the spring characteristic of parallel elastic actuators," *IEEE Robot. Autom. Mag.*, vol. 4, no. 2, pp. 854–861, Apr. 2019.

[11] C. Della Santina *et al.*, "The quest for natural machine motion: An open platform to fast-prototyping articulated soft robots," *IEEE Robot. Autom. Mag.*, vol. 24, no. 1, pp. 48–56, Mar. 2017.

[12] R. Nasiri, A. Ahmadi, and M. N. Ahmadabadi, "Realization of nonlinear adaptive compliance: Towards energy efficiency in cyclic tasks," in *Proc. 7th Int. Conf. Robot. Mechatron. (ICRoM)*, 2019, pp. 175–180.

[13] T. Marcucci, M. Garabini, G. M. Gasparri, A. Artoni, M. Gabiccini, and A. Bicchi, "Parametric trajectory libraries for online motion planning with application to soft robots," in *Robotics Research*. Cham, Switzerland: Springer, 2020, pp. 1001–1017.

[14] S. Haddadin, F. Huber, and A. Albu-Schäffer, "Optimal control for exploiting the natural dynamics of variable stiffness robots," in *Proc. IEEE Int. Conf. Robot. Autom.*, 2012, pp. 3347–3354.

[15] K. Sreenath, H.-W. Park, I. Poulakakis, and J. W. Grizzle, "A compliant hybrid zero dynamics controller for stable, efficient and fast bipedal walking on mabel," *Int. J. Robot. Res.*, vol. 30, no. 9, pp. 1170–1193, 2011.

[16] M. Khoramshahi, R. Nasiri, M. Shushtari, A. J. Ijspeert, and M. N. Ahmadabadi, "Adaptive natural oscillator to exploit natural dynamics for energy efficiency," *Robot. Auton. Syst.*, vol. 97, pp. 51–60, Nov. 2017.

[17] D. Lakatos, G. Garofalo, F. Petit, C. Ott, and A. Albu-Schäffer, "Modal limit cycle control for variable stiffness actuated robots," in *Proc. IEEE Int. Conf. Robot. Autom. (ICRA)*, 2013, pp. 4934–4941.

[18] G. Garofalo and C. Ott, "Passive energy-based control via energy tanks and release valve for limit cycle and compliance control," *IFAC PapersOnLine*, vol. 51, no. 22, pp. 73–78, 2018.

[19] G. Kerschen, M. Peeters, J. C. Golinval, and A. F. Vakakis, "Nonlinear normal modes, part I: A useful framework for the structural dynamicist," *Mech. Syst. Signal Process.*, vol. 23, no. 1, pp. 170–194, 2009.

[20] A. Albu-Schaeffer and C. D. Santina, "A review on nonlinear modes in conservative mechanical systems," *Annu. Rev. Control*, vol. 50, pp. 49–71, 2020. [Online]. Available: www.dropbox.com/s/yhc4f8nyx3ggbk2/review.pdf

[21] A. Isidori, "Lectures in feedback design for multivariable systems," in *Advanced Textbooks in Control and Signal Processing*. Cham, Switzerland: Springer, 2016.

[22] C. Nielsen and M. Maggiore, "On local transverse feedback linearization," *SIAM J. Control Optim.*, vol. 47, no. 5, pp. 2227–2250, 2008.

[23] A. Ichikawa and H. Katayama, *Linear Time Varying Systems and Sampled-Data Systems*, vol. 265. London, U.K.: Springer, 2001.

[24] H. K. Khalil, *Nonlinear Systems*, vol. 3. Upper Saddle River, NJ, USA: Prentice Hall, 2002.